

Scaling of excitations in dim erized and frustrated spin-1/2 chains

D. Controzzi¹ C. Degli Esposti Boschi² F. Ortolani^{3,2} and S. Pasini³¹ International School for Advanced Studies and INFN, Via Beirut, 1, 34100, Trieste, Italy² CNR-INFM, Research Unit of Bologna, Viale Berti-Pichat, 6/2, 40127, Bologna, Italy³ Physics Department, University of Bologna and INFN, Via Irnerio, 46, 40126, Bologna, Italy

We study the finite-size behavior of the low-lying excitations of spin-1/2 Heisenberg chains with dim erization and next-to-nearest neighbors interaction, J_2 . The numerical analysis, performed using density-matrix renormalization group, compares previous exact diagonalization results, and shows that, for different values of the dim erization parameter, the elementary triplet and singlet excitations present a clear scaling behavior in a wide range of $\epsilon = L^{-1}$ (where L is the length of the chain and ϵ is the correlation length). At $J_2 = J_{2c}$, where no logarithmic corrections are present, we compare the numerical results with finite-size predictions for the sine-Gordon model obtained using Luscher's theory. For small ϵ we find a very good agreement for $\epsilon > 4$ or 7 depending on the excitation considered.

PACS numbers: 75.10.Pq, 75.10.Jm, 11.10.Kk, 11.10.St

Spin-1/2 chains with frustration and explicit dim erization have attracted a lot of attention for their experimental relevance to spin-Peierls materials¹ as well as for their interesting theoretical properties, related, for instance, to the presence of two independent mechanisms for spin-gap generation. The difficulties in studying these systems are a consequence of the lack of quantitative analytical methods to describe their full phase diagram and of different types of limitations in the currently available numerical methods. On the one hand, with exact diagonalization one can treat at most few dozens of sites, which is inadequate when the correlation length becomes large. On the other, using the density-matrix renormalization group (DMRG) technique² it is possible to reach hundreds of sites, but the control on the quantum numbers of the excitations is much more complicated. In both cases it is difficult to reconstruct the finite-size spectrum in absence of a theory that describes the finite-size effects, especially because some excitations (like the singlet – see below) are known to have a non-monotonic dependence on the chain length L (Ref. 3). In this paper we present a detailed finite-size analysis of DMRG results for the low-energy excitations of a spin-1/2 chain with frustration and explicit dim erization, with the aim of getting a deeper theoretical understanding of the corrections due to finite L . In particular, along a specific line in parameter space, where the spin chain is described by a massive integrable quantum field theory (QFT), we compare the numerical results with analytical predictions for the finite-size scaling based on Luscher's theory^{4,5}.

The Hamiltonian of a frustrated spin-1/2 chain with explicit dim erization has the standard form

$$H = \sum_{i=1}^{L-1} \left[J \left(1 + \left(\frac{J_2}{J} \right)^i \right) S_i \cdot S_{i+1} + J_2 S_i \cdot S_{i+2} \right] + J \cdot S_L \cdot S_1 \quad (1)$$

(periodic boundary conditions are assumed in the following). For $\epsilon = 0$ one identifies two regimes. For $J_2 < J_{2c} = 0.24J$ the model is gapless and described, at low energies, by the SU(2) Wess-Zumino-Witten-

Novikov (WZNW) conformal field theory at level $k = 1$ ($SU(2)_1$), with a marginally irrelevant perturbation. When $J_2 > J_{2c}$ the marginal perturbation changes sign and induces a gap in the spectrum. In terms of operators of the WZNW theory the dim erization term is proportional to the trace of the $SU(2)$ matrix field g . Then, in the low energy limit, (1) is described by the following Hamiltonian density^{6,7}

$$H = H_{SU(2)_1} + J \cdot J + Tr g; \quad (2)$$

where $H_{SU(2)_1} = \frac{2v}{3} :J \cdot J + J \cdot J:$, J and J are the chiral $SU(2)$ currents and satisfy the level $k = 1$ Kac-Moody algebra. The coupling constants are linearly related to J_2 and ϵ : $J = (1 - J_2/J_{2c})$ and $v = \epsilon/J$. It should always be kept in mind that, roughly speaking, the field theory description is valid if the masses are much smaller than the bandwidth, that implies $\epsilon \ll 1$ or, for $\epsilon = 0$, $(J_2 - J_{2c})/J \ll 1$.

The theory (2) is integrable when one of the two coupling constants vanish. For $\epsilon = 0$ excitations are massive (massless) spinons for $\epsilon < 0$ ($\epsilon > 0$). When $\epsilon \neq 0$, the strongly relevant perturbation $Tr g$ introduces a coupling interaction between the spinons that are no longer fundamental excitations of (2)^{8,9}. For $\epsilon = 0$ the model is again integrable and equivalent to the sine-Gordon (SG) model, $L = 1/2(\pi/v)^2$, $g = (2^2v) \cos(\pi/v)$, at $\epsilon^2 = 2$, and the spectrum contains triplet and singlet excitations^{7,10}. The ratio between their masses, $R = m_s/m_t$, is known exactly to be $R = \sqrt{3}$.

The behavior of R for finite values of ϵ (and $\epsilon \neq 0$) is difficult to address analytically even in the regime of validity of the field theory description, because (2), like its lattice counterpart (1), is not integrable. This problem was studied using exact diagonalization in Ref. 3, where it was found that the singlet is stable for any $J_2 < J_{2c}$ and R interpolates between $\sqrt{3}$ at $J_2 = J_{2c}$ and $R = 2$ at $J_2 = 0$. These results are reproduced by our DMRG analysis, although we do not report them here (see however Ref. 11 for the extension to $J_2 < 0$). Some analytical predictions can be made in the vicinity of the two integrable

points, where a perturbative analysis can be carried on¹². The vicinity of $J = 0$ is the simplest to study because the operator $J - J$ induces changes in the spectrum that are adiabatic in J (see Ref. 9). The effect of the operator T_{rg} is more difficult to take into account since continuum is a non-perturbative effect. For $J < 0$, $J > 1$ and energies close to the two-spinon threshold the continuum can be studied solving the two-particle eigenvalue problem for the two-spinon bound state⁸: The original two-spinon continuum is replaced by discrete levels, solutions of the eigenvalue equation for a linear potential, and for small J many excitations appear in the spectrum. A similar feature (additional triplet) was observed also in Ref. 3.

For the analysis of the above problem as well as many others it is essential to have a theory for the finite-size scaling that allows one to extrapolate numerical results. For massive integrable QFTs it is possible to express the leading finite-size corrections to the spectrum in terms of their exact scattering data^{4,5}. As we recalled, there are two points for which (2) is integrable. In this paper we consider the integrable point $J = 0$ and $J \neq 0$, rather than $J = 0$ and $J < 0$, because the former case presents bound states and is physically more interesting. Numerically this is also the easiest scenario to investigate because in the other case the gap opens very weakly¹³. Hence, in the following we will compare DMRG data for the lattice Hamiltonian (1) with $J_2 = J_{2c}$ and $J > 1$ with predictions coming from the SG theory at $J^2 = 2$.

Let us start presenting the numerical results. Before studying the finite-size effects we extract from the numerical data some important non-universal pre-factors of a problem recently addressed in Ref. 14. It is well known that, in absence of logarithmic corrections, the triplet mass scales as $M_t = A_t^{2/3}$, with A_t being a non-universal amplitude. The energy gaps, computed with DMRG, are linearly related to the masses through a velocity pre-factor that we express as $v = C_v J = 2: E_t = v M_t$ (the lattice spacing is formally set to one). For $J_2 = 0$ it is known that $C_v = 1$, but for $J_2 = J_{2c}$ the constant may assume a different value. Another unknown constant connects v with the coefficient of the relevant term in the SG model: $g_1 = 6J = 2^{1/4}C$ ($C = 1$ for $J_2 = 0$ ¹⁴). Along the same lines of Ref. 14 we can extract these constants from the pre-factors of the triplet gap and ground-state energy density, that we write as $E_t = J = 1:723K_t^{2/3}$ and $E_{\text{gs}}(0) = J = 0:2728K_{\text{gs}}^{4/3}$, respectively. The relation between the constants is $K_t = C_v (C = C_v)^{2/3}$ and $K_{\text{gs}} = C_v (C = C_v)^{4/3}$. We have computed these quantities for some values of J using the finite-system DMRG algorithm² with three "zips" in a range of L from 10 to 100. The results are presented in Table I, and imply $C_v \approx 0:81$ and $C \approx 1:53$ at $J_2 = J_{2c}$, to be compared with $C = C_v = 1$ at $J_2 = 0$.

Let us now come to the central part of the paper by examining the finite-size features of the low-energy spectrum. In the framework of the DMRG this is done by building the superblock density matrix as a mixture (with equal weights) of the matrices associated with a

	$E_t = J$	K_t	K_{gs}	$v_1 = J$	$L_{\text{min}}()$
0.01	0.09875	1.235	1.966	1.1921	50
0.02	0.15705	1.237	1.948	1.1822 0.0010	30
0.10	0.46233	1.245	1.800	1.1425 0.0003	10

TABLE I: Triplet gaps, constants K_t , K_{gs} and estimates of the "1-particle velocity" v_1 for different values of J and $J_2 = J_{2c}$ (see text after Eq. (10) for the determination of $E_t = J$). Typically $M = 256$ optimized DMRG states have been retained. When $E_t < 0:1$ we have improved the precision using $M = 405$. The last column contains the (approximate) values of L at which the singlet gaps attain a minimum.

prescribed number of target states. By means of the thick-restart variant of the Lanczos method¹⁵ we are able to target up to ten excited states in each sector of $S_{\text{tot}}^z = \sum_i S_i^z$, which is the only good quantum number that we have exploited. First of all from the so-called 1-particle (1P) excitations of the triplet we can get an independent estimate of the velocity. In fact, these excitations for small momenta $q_p = 2\pi/L$ (with $n = 1, 2, \dots$) have energy $E_p = E_{\text{gs}} + E_t^2 + v_1^2 q_p^2$. So we have checked that $E_n^2/E_t^2 = 2$ actually scale as $n v_1$ and we have reported the values of v_1 in Table I. Unfortunately, these states with nonzero momentum represent also the main limitation that we have encountered in the computation of the singlet gap E_s at large values of L . This is because all the excited states that we can target in $S_{\text{tot}}^z = 0$, say N_0 , are eventually exhausted by the triplet and its 1P excitations. In practice, the singlet "disappears" from the set of DMRG levels for $L > (N_0 - 2) v_1 = E_t R^2 \approx 1$, where R is the mass ratio¹⁶. In addition, unlike the triplet, the singlet level has a non-monotonic dependence on L . Typically $E_s(L)$ decreases with increasing L up to a characteristic value $L_{\text{min}}()$, beyond which it starts to increase and converges to the asymptotic limit from below. An example of such a feature is plotted in Fig. 1 for $J = 0:02$ and $J_2 = J_{2c}$. As listed in Table I the values of L_{min} increase for $J > 0$ so that there exists a minimum value of L below which L_{min} becomes larger than the maximum reliable size that we can handle with the DMRG.

There are other cases in the literature for which numerical results show that some states in the spectrum exhibit a non-monotonic dependence on L (see for instance Ref. 17). In such situations it is particularly difficult to get a reliable estimate of the finite-size value. In some cases it is possible to push L beyond the minimum and even beyond the L where the finite-size data start to saturate. Whenever this is not the case one should use a suitable fitting function that displays the "bump" and the convergence from below for some choice of the fitting parameters. For example, Eq. (6) in Ref. 3 captures reasonably well the essential features in most of the cases, but we are not aware of any theoretical justification. Hence, in the following we will study the finite-size corrections to the masses in a field-theoretic framework where, for large L , the scaling function can be computed

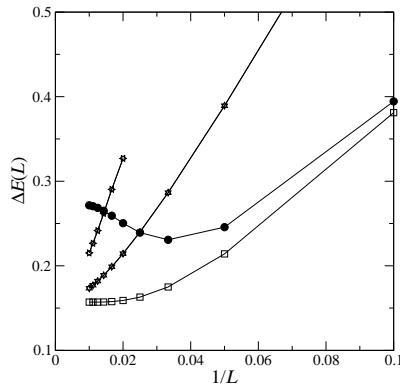


FIG. 1: Finite-size gaps vs $1/L$ for $= 0.02$ and $J_2 = J_{2c}$: triplet (open squares), singlet (full circles), lowest 1P triplet excitations with momenta different from 0 and (coinciding up and down triangles). Following the singlet at large L requires to target various excited states within $S_{\text{tot}}^z = 0$ ($N_0 = 6$ in this example, where $M = 256$), due to the crossing with 1P states. The singlet curve has a minimum at L_m in $(0.02) \sim 30$.

with no fitting parameters.

As already recalled for $J_2 = J_{2c}$ and $= 1$ the spin chain is described by the integrable SG model at $\beta^2 = 2$. The factorized scattering theory explicitly shows the hidden $SU(2)$ symmetry of the model at this point⁷. The spectrum consists of a soliton s and an anti-soliton \bar{s} which are degenerate with a breather state b_1 . Moreover, all these particles have the same S-matrix^{7,10}

$$S_{a;b}(\beta) = S_0(\beta) = \frac{\sinh \beta + i \sin \beta}{\sinh \beta - i \sin \beta} = ; \quad a;b = s; s; b_1 : \quad (3)$$

The rapidity parameterizes the relativistic dispersion relations: $e_a = m_a \cosh \beta$, $p_a = m_a \sinh \beta$. In addition, there is another breather state b_2 of higher mass. The additional S-matrices are^{7,10}

$$S_{a;b_2}(\beta) = S_0(\beta + i\beta = 6)S_0(\beta - i\beta = 6); \quad a = s; s; b_2; \quad (4)$$

$$S_{b_2;b_2}(\beta) = [S_0(\beta)]^3; \quad (5)$$

The excitations can be then organized into a triplet ($s; s; b_1$) of mass m_t and a singlet of mass $m_s = \sqrt{3}m_t$.

For what follows, it is worth recalling that bound states, like the breathers, are associated to poles in the S-matrix. In particular if $\beta = i\beta_{bc}^a$ is a pole in the scattering process of the particle b and c the mass of the bound state is given by: $m_a^2 = m_b^2 + m_c^2 + 2m_b m_c \cos \beta_{bc}^a$. For instance, the simple poles in the S-matrix $S_{s;s}(\beta)$ at $\beta = 2i\beta = 3$ and $\beta = i\beta = 3$ correspond to the two breathers (it is easy to check their masses are m_t and m_s respectively). The third order pole at $\beta = 2i\beta = 3$ in $S_{b_2;b_2}(\beta)$ should be interpreted as associated to intermediate virtual particles in the scattering processes¹⁸, as drawn in Fig. 2. All other poles in (3-5) are redundant and do not correspond to additional bound states¹⁰.

The finite-size corrections for a QFT in a large but finite volume with periodic boundary conditions are a consequence of the vacuum polarization and, when the

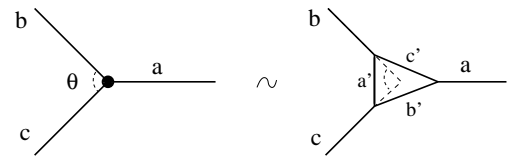


FIG. 2: Physical interpretation of third order poles. The angle θ is related to the poles in the intermediate processes as $= u_{b;a}^{c^0} + u_{c;a}^{b^0}$.

model is integrable, they can be extracted from the exact scattering data of the infinite-volume theory^{4,5}. The leading corrections to the masses are exponentially small and consist of two terms

$$m_a(L) = m_a^{(F)}(L) + m_a^{(1)}(L); \quad (6)$$

which roughly can be understood as follows. The first term exists in any theory and can be interpreted as virtual particles "traveling around the world" once before being annihilated again. It has the form

$$m_a^{(F)}(L) = \sum_b \frac{d}{2} e^{e_b(\beta)L} e_b(\beta) f_{a;b}(\beta); \quad (7)$$

where $f_{a;b}(\beta) = S_{a;b}(\beta + \frac{i}{2}) - 1$. For large L Eq. (7) is of order $O(e^{m_b L})$. The second term in (6) is present only in theories with bound states and is associated to virtual processes in which a particle is split into its two constituents that "travel around the world" before recombining again into the original particle. If the particle a is bound state of two other particles of the theory, say $b; c$, associated to the pole $\beta = i\beta_{bc}^a$, then $m_a^{(1)}(L)$ reads

$$m_a^{(1)}(L) = \sum_{b;c} m_a^2 \mathcal{H}_b^2 m_c^2 j_{abc} R_{abc} e^{i\beta_{bc}^a L}; \quad (8)$$

where \mathcal{H} denotes the Heaviside step function and

$$j_{abc} = m_b \sin u_{ab}^c; R_{abc} = i \text{Res}_{\beta = i\beta_{bc}^a} S_{a;b}(\beta); \quad (9)$$

As mentioned before the third order pole has to be interpreted as formation of virtual particles and $R_{abc} = R_{ab} R_{bc} R_{ca}$. In general, since for small L , $E_{\text{size}}(L) \sim 1/L$, if the terms above approach the infinite-volume limit from below the scaling function will present a minimum (the minimum may also appear as a consequence of the competition of the two terms in (6)⁵).

Since the singlet and the triplet masses are related, all the finite-size corrections depend on the scaling variable $m_t L$. It should be noticed that the integrals in (7) involving $f_{a;b}(\beta)$, with a belonging to the triplet, diverge and need to be regularized. Such divergences are possible in one dimensional models, but there is no general prescription to treat them⁵. We regularized them by simply subtracting the divergent part. In any case, it turns out that the contribution from this term (not shown below) is very small and then the choice of the regularization

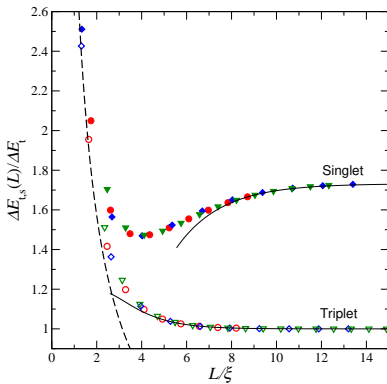


FIG. 3: Scaling plot of finite-size corrections to the triplet and singlet gaps $E_{s,t}$ at $J_2 = J_{2c}$. Continuous lines represent the analytical predictions (10) and (11), while the symbols refer to DMRG data obtained with the same parameters as in Table I (circles: $\epsilon = 0.01$; diamonds: $\epsilon = 0.02$; triangles: $\epsilon = 0.10$). The dashed line shows the $1/\xi$ behavior at small ξ .

scheme does not affect the analysis. Using formulae (6-8) and the pole structure of the S-matrix, we find the following expression for the leading finite-size corrections, $E_{s,t}(L) = E_t(1)$,

$$E_t(1) = 1 + 6e^{-\frac{p}{3-2}} \left(3 - \frac{1}{2} \right) e^{-\frac{p}{3} \cosh f_0(1)}; \quad (10)$$

$$E_s(1) = \frac{p}{3} - 1 - 3e^{-\frac{p}{2}} - 36e^{-\frac{p}{3}}; \quad (11)$$

with $f_0(1) = \frac{p}{2} \cosh^{-1} \left(\frac{2}{3} \cosh^{-1} \frac{p}{3} \right)$. These scaling functions are compared to the scaled DMRG data in Fig. 3 (one has to replace $m_t L$ with the scaling variable $\xi = L/\xi$). For each value of the scale factors (slightly different for triplet and the singlet) and E_t have been tuned in order to give the best collapse of

the curves. Using the numbers found for the triplet, the product $v = E_t$ yields another estimate of the velocity, $v = 1.19 \pm 0.01$, in agreement with those in Table I.

A first interesting result of this analysis is that stable excitations of the lattice model at $J_2 = J_{2c}$ perturbed by the dimersization term exhibit a clear scaling behavior over the whole range of L for different values of ϵ . Moreover, it is seen that Lüscher's corrections of the SG model with $\epsilon^2 = 2$ capture well the finite-size effects of the spin Hamiltonian for $\epsilon > 4$ or 7, depending on which of the two excitations we consider. In these regimes they do not have the empirical form that is usually assumed¹⁹.

Finally, we have repeated the numerical analysis for other values of J_2 , and the scaling plots are qualitatively similar to Fig. 3. Unfortunately in this case the low-energy effective field theory is no longer integrable and computations of finite-size corrections are much more difficult. Nevertheless both the variation of the mass and of the S-matrix can be taken into account perturbatively¹². Interestingly enough, our numerical results show that for the triplet gap the scaling function (10) does a good job also for $J_2 > J_{2c}$ once the gaps and L are suitably rescaled. On the other hand, for the singlet, there still exist an approximate collapse of the numerical data on a single scaling curve but, even in the regime of large ξ , we do not have a satisfactory analogue of the function $E_s(1)$.

We would like to thank G. Mussardo for suggesting to compare the DMRG results with Lüscher's theory and for essential discussions. D.C. thanks A.N. Mersyany for important discussions and interest in the work. We also acknowledge useful observations made by E. Ercolessi, G. Morandi, M. Roncaglia, L. Campos Venuti and G. Delno. This work was partially supported by the TMR network EUCLID (HPRN-CT-2002-00325), and by the Italian MIUR through COFIN projects (prot. n. 2002024522_001 and 2003029498_013).

- ¹ M. A. in et al., Phys. Rev. Lett. 78, 1560 (1997); M. W. Eiden et al., Z. Phys. B 103, 1 (1997); M. Fischer et al., Phys. Rev. B 60, 7824 (1999).
- ² S. R. White, Phys. Rev. B 48, 10345 (1993).
- ³ G. Bouzerar, A. P. Kampf and G. I. Japaridze, Phys. Rev. B 58, 3117 (1998).
- ⁴ M. Lüscher, Commun. Math. Phys. 104, 177 (1986).
- ⁵ T. R. Klassen and E. Melzer, Nucl. Phys. B 362, 329 (1991); V. P. Yurov, A. B. Zamolodchikov, Int. J. Mod. Phys. A 5, 3221 (1990).
- ⁶ I. A. Eck and F. D. M. Haldane, Phys. Rev. B 36, 5291 (1987).
- ⁷ I. A. Eck, Nucl. Phys. B 265, 448 (1986).
- ⁸ I. A. Eck, in Dynamical properties of unconventional magnetic systems, Kluwer Academic Publishers (1997) and cond-mat/9705127.
- ⁹ D. Controzzi and G. Mussardo, Phys. Rev. Lett. 92, 021601 (2004); Phys. Lett. B 617, 133 (2005).
- ¹⁰ A. B. Zamolodchikov and Al. B. Zamolodchikov, Ann. Phys. NY 120, 253 (1979).
- ¹¹ L. Campos Venuti et al., J. Stat. Mech. (2005), L02004.

¹² G. Delno, G. Mussardo and P. Simonetti, Nucl. Phys. 473, 469 (1996).

¹³ R. Chitra et al., Phys. Rev. B 52, 6581 (1995).

¹⁴ E. O. Rignac, Eur. Phys. J. B 39, 335 (2004).

¹⁵ For the original algorithm see: K. Wu and H. Simon, SIAM J. Matrix Anal. Appl. 22, 602 (2000); For the implementation into the DMRG see: C. D'egli Esposti Boschi and F. Ortolani, Eur. Phys. J. B 41, 503 (2004).

¹⁶ This formula stems from equating $E_s = R E_t$ to the energy of the highest 1P state with momentum $\mathbf{q} = 2 = L/N_0 - 2 = 2$, given that within the N_0 states we have to include the singlet, the triplet and all the 1P excitations that are doubly degenerate in momentum.

¹⁷ J. Z. Zhao, et al., Phys. Rev. Lett. 90, 207204 (2003); J. Lou et al., Phys. Rev. B 68, 045110 (2003).

¹⁸ S. Coleman and H. J. Thun, Commun. Math. Phys. 61, 31 (1986); C. J. Goebel, Progr. Th. Phys. Suppl. 86, 261 (1986).

¹⁹ T. Barnes et al., Phys. Rev. B 47, 3196 (1993).